LAWRENCE
LIVERMORE
NATIONAL
LABORATORY

LLNL-JRNL-607756

Numerical Study of the Sensitivity of X-Ray Driven Implosions to Low-Mode Flux Asymmetries

R. H. Scott, D. S. Clark, D. K. Bradley, D. A. Callahan, M. J. Edwards, S. W. Haan, O. S. Jones, B. K. Spears, M. M. Marinak, R. PJ. Town, P. A. Norreys, L. J. Suter

December 11, 2012

Physical Review Letters

Disclaimer

This document was prepared as an account of work sponsored by an agency of the United States government. Neither the United States government nor Lawrence Livermore National Security, LLC, nor any of their employees makes any warranty, expressed or implied, or assumes any legal liability or responsibility for the accuracy, completeness, or usefulness of any information, apparatus, product, or process disclosed, or represents that its use would not infringe privately owned rights. Reference herein to any specific commercial product, process, or service by trade name, trademark, manufacturer, or otherwise does not necessarily constitute or imply its endorsement, recommendation, or favoring by the United States government or Lawrence Livermore National Security, LLC. The views and opinions of authors expressed herein do not necessarily state or reflect those of the United States government or Lawrence Livermore National Security, LLC, and shall not be used for advertising or product endorsement purposes.

Numerical Study of the Sensitivity of X-Ray Driven Implosions to Low-Mode Flux Asymmetries

R.H.H. Scott,[1,*] D.S. Clark,[2] D.K. Bradley,[2] D.A. Callahan,[2] M.J. Edwards,[2] S.W. Haan,[2] O.S. Jones,[2] B.K. Spears,[2] M.M. Marinak,[2] R.P.J. Town,[2] P.A. Norreys,[1,3] and L.J. Suter[2]

[1] *Central Laser Facility, STFC Rutherford Appleton Laboratory, Harwell Oxford, Didcot, OX11 0QX, United Kingdom*

[2] *Lawrence Livermore National Laboratory, Livermore, CA 94551, United States of America*

[3] *Department of Physics, University of Oxford, Parks Road, Oxford OX1 3PU, United Kingdom*

(Dated: November 30, 2012)

Abstract

The sensitivity of inertial confinement fusion implosions of the type performed on the National Ignition Facility (NIF) [1] to low-mode flux asymmetries has been investigated numerically. It is shown that large-amplitude, low-order mode shapes (Legendre polynomial P_4), resulting from associated low order flux asymmetries, cause spatial variations in capsule and fuel momentum that prevent the DT "ice" layer from being decelerated uniformly by the hot spot pressure. This reduces the transfer of kinetic to internal energy of the central hot spot, thus reducing neutron yield. Furthermore, synthetic gated x-ray images indicate that the P_4 component of hot spot self-emission shape is insensitive to P_4 hot spot shapes, and a positive P4 asymmetry aliases itself as a negative or oblate P2 in these images. Correction of this apparent P_2 distortion can further distort the implosion while creating a round x-ray image. Long wavelength asymmetries may be playing a significant role in the observed yield reduction of NIF DT implosions relative to detailed post-shot 2D simulations.

Indirect-drive inertial confinement fusion (ICF) [1–3] uses lasers to heat the inside of a cavity (or hohlraum). The absorbed laser energy is re-emitted as approximately black-body radiation in the soft x-ray regime. These x-rays heat the outer surface of a hollow, spherical, ~ 2 mm diameter, shell that contains a ~ 70 µm thick layer of cryogenically frozen Deuterium and Tritium fuel ("DT fuel" or "DT layered capsules"). The heated outer shell ablates, which creates a reaction force, accelerating the remaining shell spherically inwards at extremely high velocity ($\sim$ 350 km/s). During the implosion, spherical convergence causes the pressure in the gaseous void (or hot spot) within the shell to rise rapidly. This pressure decelerates the shell, simultaneously compressing the solid fuel and converting the shell's kinetic energy into hot spot internal energy. If this conversion rate exceeds loss rates due to thermal conduction and bremsstrahlung radiation, the hot spot will heat, initiating DT fusion reactions. Provided the hot spot areal density is sufficient, α-particles created by the fusion reactions will redeposit their energy locally, further heating the hot spot, resulting in bootstrap heating, ignition, and propagation of burn into the surrounding cold fuel. Numerical modeling indicates that the National Ignition Facility (NIF) can, for the first time, initiate inertial fusion ignition in the laboratory [4–6].

In this Letter, the effects of large, low-mode asymmetries in the x-ray drive are examined numerically. The non-uniformity of the x-ray flux incident upon the shell and the resultant non-spherical shell shapes can be described mathematically as a series of Legendre polynomials [7]. It is shown that a P_4 implosion asymmetry, that might result from low-order hohlraum generated flux asymmetries, causes spatial variations in the capsule and fuel momentum. This can inhibit the DT fuel from being decelerated uniformly by the hot spot pressure, reducing the efficient transfer of implosion kinetic energy to hot spot internal energy thus significantly reducing the capsule performance. Furthermore, simulated gated x-ray images of the hot spot self-emission show reduced sensitivity to the P_4 mode, instead the images appear to have a P_2 shape. Reducing the amplitude of an oblate P_2 shape caused by a positive P_4 mode (as measured from the x-ray image) further reduces the sensitivity to the P_4 mode making a quantitative evaluation of the hot spot a_4 (where a_4 is the amplitude of the P_4 mode) ambiguous. Correcting the apparent P_2 in the x-ray image can in fact cause the capsule shape to be highly distorted. Comparisons are made between key physical properties of the implosion, synthetically generated experimental observables, and NIF experimental data.

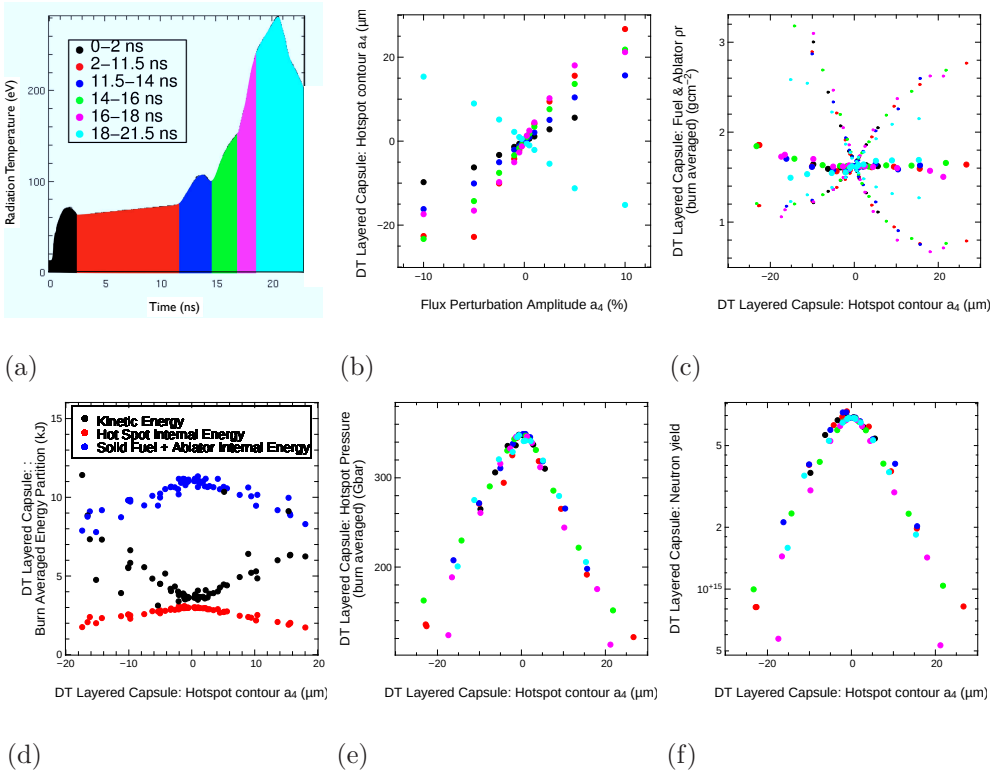

Figure 1. (a) Applied radiation temperature vs time. Colors depict when during the drive pulse the various flux asymmetries were applied as shown on subsequent plots. (b) The relationship between applied flux asymmetry and hot spot a_4 at x-ray bangtime (the time at which peak emission occurs). Each point represents a 2D Hydra run. (c) Burn averaged hot spot + fuel + ablator ρr vs hot spot a_4 at x-ray bangtime: large dots are spatially averaged ρr, while the smaller points with the same color and a_4 are the maxa and minima of the spatially averaged value; large variations in ρr occur due to P_4. (d) The burn averaged energy partition as a function of hot spot a_4; increasing P_4 perturbations prevent kinetic energy (black) from being converted to both hot spot (red) and solid fuel (blue) internal energy during stagnation. (e) Burn averaged hot spot pressure as a function of hot spot a_4. (f) Total thermonuclear neutron yield as a function of hot spot a_4; yield varies by a factor of 15.

The indirect-drive approach to ICF smooths high mode spatial non-uniformities in the x-ray flux incident on the capsule, however the spatial distribution of the cones of laser beams which illuminate the hohlraum means that low mode x-ray flux non-uniformities can occur [1], these are considerably lower mode than those recently examined by Thomas *et al* [8]. The growth of Legendre polynomial P_4 capsule shapes was investigated using the

radiation-magnetohydrodynamics code Hydra [9]. A frequency and time dependent x-ray source was developed to drive these capsule-only simulations. The initial x-ray drive was taken from an integrated hohlraum simulation and then adjusted to match the shock timing data obtained using the VISAR diagnostic [10] from NIF shot N110521, and the capsule implosion trajectory [11] measured on NIF shot N110625. A 90° 'wedge' of the capsule (2π Sr) was modeled using two-dimensional (2D) cylindrically-symmetric geometry with 256×312 cells. Doubling and quadrupling the cell resolution demonstrated convergence. In all runs the Quotidian Equation of State [12] was used with tabular opacities and multi-group radiation diffusion. The effects of Legendre polynomial P_4 hohlraum flux asymmetries were investigated by perturbing the tuned x-ray drive with spatially varying flux asymmetries of the form: $fds(\theta, t) = (a_0 P_0 + a_4 P_4(\theta)) * fds(t)$ where fds is the energy density of the tuned photon frequency dependent x-ray drive source, a_n is the amplitude of the nth Legendre polynomial, $a_0 = 1$, $a_4 = (\pm 0.10, \pm 0.05, \pm 0.025, \pm 0.01, \pm 0.005, \pm 0.0025)$, θ the angle between the equatorial plane and polar axis, and t time. The P4 asymmetries applied in this sensitivity study extend beyond what is nominally expected in NIF ignition hohlraums. Hydra modeling of the hohlraum and capsule suggests the flux asymmetry incident on the capsule would be expected to vary by $< 3\%$ except for in the first ~ 1 ns of the laser pulse were it can vary by up to 10% [13]. The flux asymmetries were applied 100 µm from the capsule ablation front during discrete time intervals (see fig. 1(a)), creating a database of > 200 2D modeling runs of both DT layered implosions and DHe^3 gas filled capsules with a surrogate inner CH layer of equal mass to a DT fuel layer (symmetry capsules). Time resolved synthetic gated x-ray images of the hot spot self-emission > 6 keV, including its attenuation by the compressed fuel and ablator, were created from both polar and equatorial directions by post processing each Hydra run. The images were blurred in order to reproduce the 11 µm resolution of the diagnostic. The key implosion performance metrics (neutron yield, hot spot pressure, mass, volume, density, ion and electron temperatures, the effective ion temperature computed from the FWHM of the DT neutron spectrum, fuel and ablator areal density (ρr) and kinetic energy) were extracted from the simulations. The hot spot shape was evaluated as a function of time by performing a Legendre polynomial decomposition (modes 1-10) of the appropriate contour. For DT layered capsules the hot spot contour is defined for each angular 'strip' of cells j as the minimum radius where $T_{e_j} > \frac{1}{2} T_{e_{j_{max}}}$ and $\rho_j < \frac{1}{2} \rho_{j_{max}}$ where T_e is the electron temperature and ρ the mass density,

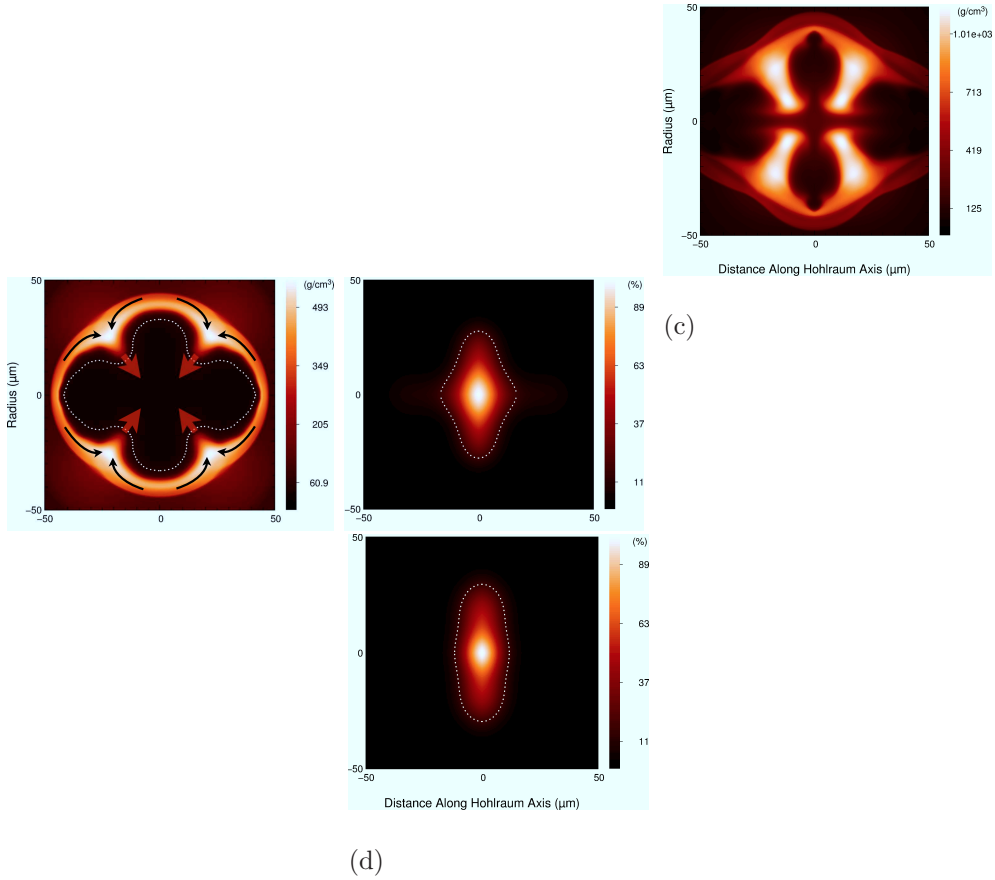

Figure 2. Axis of rotational symmetry is horizontal at Radius = 0 μm. (a) DT layered capsule density plot at x-ray bangtime showing a positive Legendre polynomial P_4 shape. This simulation had a 10% flux asymmetry applied during the second shock (11.5-14 ns). Black arrows indicate the mass flows which occur during stagnation. After bangtime 'fingers' of fuel continue to flow inwards (red arrows). White dots depict the hot spot contour. (b) Synthetic gated x-ray image of the hot spot self emission from (a), white dots show the 17% contour. (c) Fig. (a) 100 ps later: due to burn truncation with large a_4 this is the neutron bangtime for an equivalent spherical implosion. (d) The synthetic GXD from (c), showing a large negative P_2 and almost zero a_4 despite the obvious P_4 in (c).

'max' denotes the maximum value within the jth strip. This has been found to produce a robust definition of the hot spot even for highly distorted implosions. The 17% contour of the gated x-ray diagnostic (GXD) is used both for the synthetic GXD and experimentally, as previous studies have shown this provides a faithful representation of the hot spot shape for small departures from sphericity.

The applied Legendre P_4 flux asymmetries induce P_4 hot spot shapes at stagnation (see Figs. 2 (a) and (c)), the sign of which is dependent on the timing of the applied flux asymmetry. If the asymmetry is present only during the shock compression phase (the first $\sim$ 18 ns), shocks created in regions of the capsule exposed to higher flux propagate faster, these faster shocks break out of the inner DT ice layer earlier, causing these regions to move ahead of those exposed to less flux. This also causes ablator mass to flow laterally, away from the high flux region. Consequently during peak drive the regions initially exposed to high flux are at smaller radii, meaning they are accelerated less efficiently by the hohlraum flux and gain less total momentum. They can also have less ablator aerial density. The net effect is that the regions experiencing high flux during shock compression will protrude outwards at stagnation. Conversely if the flux asymmetry is applied during peak drive, the regions of the capsule exposed to more flux gain more momentum, and protrude inwards at stagnation. Regardless of the timing of the applied asymmetry, during the stagnation phase of the implosion, pressure within the lower density hot spot decelerates the higher density fuel from peak velocity, making this interface Rayleigh-Taylor unstable [14, 15]. The instability will accentuate any shape imperfections during deceleration, as indicated by the significant simulated growth shown in figs. 2(a) and (c).

The scalings of some important DT layered capsule implosion parameters as a function of hot spot a_4 measured at x-ray bangtime are summarized in figure 1. Fig. 1(b) shows the relationship between applied P_4 flux perturbation amplitude and the resulting shape a_4 at x-ray bangtime. Fig. 1(c) depicts the 'burn averaged' ρr (the burn average of a quantity $Q_b = (\sum_{t=0}^{t=\infty} Q_t Eprodrdt)/\int_{t=0}^{t=\infty} Eprodr\ dt$ where Q_t is Q at time t and $Eprodr$ the thermonuclear energy production rate in time dt) as a function of hot spot a_4. Although the spatially averaged ρr is relatively constant, the lateral mass flows caused by the P_4 can create large spatial variations in ρr. The regions with higher momentum continue to propagate radially inwards; fig. 1(d) depicts the remaining capsule kinetic energy as a function of a_4 and the partitioning of total energy into hot spot and solid fuel internal energy. For large a_4 less of the implosion kinetic energy is converted into hot spot internal energy and the hot spot pressure is reduced (see fig. 1(e)). The reduction in neutron yield can be as large as 15$\times$ for hot spot $a_4 = 20$ µm (achieved by applying a flux asymmetry of $\sim$ 10%) as shown in fig. 1(f)).

Analysis of synthetic GXD images created from the 2D Hydra runs suggest that the a_4

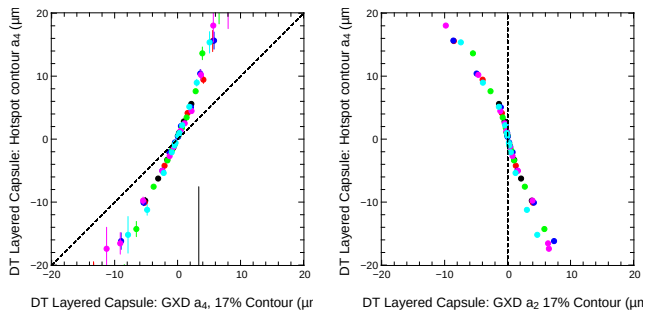

(a) (b)

Figure 3. (a) DT layered capsule hot spot a_4 plotted against the synthetic GXD a_4; particularly for large positive a_4 the GXD is unable to effectively measure the amplitude of the P_4 mode. (b) DT layered capsule hot spot a_4 plotted against the synthetic GXD a_2; the GXD measures a significant P_2 mode amplitude despite the DT layered capsule hot spot a_2 being 0 ± 1 µm (not shown).

measured experimentally with the GXD is not a true representation of the hot spot a_4, particularly for large positive a_4 amplitudes. Fig. 3(a) depicts the relationship between the DT layered capsule "hot spot a_4" (as previously defined) and that from the 17% contour of the synthetic GXD (the synthetic GXD a_4), both were extracted at x-ray bangtime (the principal value used for analysis of experimental data). The absolute value of the a_4 measured from the synthetic GXD is consistently smaller than that of the hot spot. The insensitivity to positive hot spot a_4 is caused by lateral ablator mass flows which accumulate at $\sim 45°$ at the expense of ablator material near the equator and poles (see Fig. 2 (a)). The ablator material is rotationally symmetric about the horizontal axis, so the accumulated material absorbs the x-rays emitted from the polar-lobes of the hot spot (left and right), while allowing x-rays to more readily pass through the equatorial regions (top and bottom). Consequently the polar-lobes of the hot spot which are visible in the density plots of Fig. 2 as dark regions (the hot spot is the central region of low density) are almost completely invisible in the GXD plots compared to the emission through the equator. This causes the x-ray image to have a negative P_2 shape (oblate or "pancaked"). As the hot spot $a_2 = 0 \pm 1$ µm (a_2 is the amplitude of the P_2 mode) for all these pure P_4 modelling runs, the P_2 inferred from the x-ray image is a "false" P_2 mode. This suggests that a negative P_2 mode measured from the self-emission x-ray image may in fact be a signature of a positive P_4 mode, although it does not, of course, preclude the presence of a true P_2 mode. This is potentially important for interpretation of x-ray images from DT implosions, which often exhibit oblate (negative)

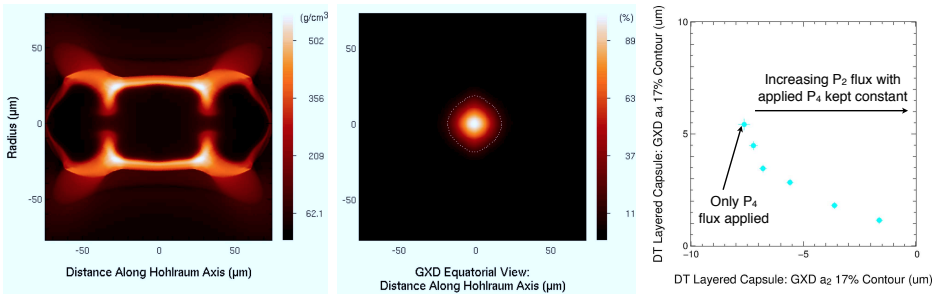

Figure 4. (a) Density plot of a DT layered capsule run with both P_2 and P_4 flux modes applied. Axis of rotational symmetry is horizontal at Radius = 0 µm. (b) The equatorial synthetic GXD image of (a) at the same time, dotted line shows 17% contour. Despite the highly non-spherical density distribution, the equatorial GXD image is almost perfectly round. (c) As the P_2 flux amplitude is increased in order to make the GXD image look round (reducing a_2) the sensitivity to a_4 is reduced towards zero.

P_2 modes [18].

NIF experiments also use low convergence, DHe^3 gas filled "symmetry capsules" which have a surrogate CH fuel mass. Using Hydra, symmetry capsule and DT layered capsule pairs of runs were created by applying identical x-ray drives to both capsules. These calculations indicate symmetry capsules also show reduced sensitivity to a_4, exhibit a "false" P_2, and are quantitatively very similar to those shown in Figs. 3 (a) and (b) respectively.

DT implosions on the NIF currently have yields $\sim 3-10\times$ below detailed 2D post-shot Hydra simulations [19] that match the measured shock timing, implosion velocity, and capsule and ice surface roughnesses. In comparison to experimentally measured or inferred values [20], detailed post-shot simulations have similar hot spot temperatures, however the hot spot volumes are reduced while the hot spot mass is increased, causing a $2-3\times$ discrepancy in the hotspot density. P_4 shape perturbations offer one mechanism which may explain these experimental observations in particular bringing the yield and ion temperature relationship into better agreement. In these simulations, the DT fuel and hot spot do not mix; clear boundaries still exist (note these simulations use smooth capsules, but when nominal realistic capsule surface roughness [16] was employed and modes up to 200 resolved, no significant implosion degradation occurred for the full range of a_4). Consequently unlike high mode 'mix' [1] (where the hot spot can be radiatively cooled by high Z impurities), the simulated ion temperature inferred from the neutron spectrum remains unaffected at 3.9 ± 0.05

	NIF expt. range[20]	Hydra ($a_4 = 0$ µm)	Hydra ($a_4 = 20$ µm)
Pressure (GBar)	57-81	348	115
Mass (µg)	2-6.4	8	5.5
Density (gcm^{-3})	22-35	136	69
Volume ($\times 10^{-7} cm^3$)	0.9-1.9	0.6	1.0
Tion (keV)	3.3-4.4	3.9	3.9
Fuel ρr (gcm^{-2})	0.77-0.98	0.7	0.72
Yield (neut. $\times 10^{14}$)	1.9-6.0	74	5.3

Table I. A comparison of NIF DT layered capsule experimental data from 4 shots N110608-N110908 with two Hydra implosions, one spherical ($a_4 = 0$ µm, and another with $a_4 = 20$ µm. Large positive P_4 brings the modeled implosion observables approximately in line with the experimental data.

keV for all a_4. The large a_4 does however truncate the thermonuclear burn, moving both the neutron and x-ray bangtimes earlier in time, increasing the measured hot spot volume. The hot spot mass decreases with positive a_4, bringing Hydra simulations approximately in line with experimental data, as shown in Table I. This compares NIF experimental data [20] with two Hydra implosions; one is perfectly spherical while the other has a hot spot a_4 of +20 µm. Notable features are reduced yield, pressure and hot spot mass, while leaving the ion temperature and increasing the hot spot volume. We must emphasize, however, that this should not be interpreted as conclusive evidence that a P_4 asymmetry is responsible for the observed reduced NIF capsule performance. Although this study has concentrated on the P_4 mode, it is likely that all low modes would reduce the conversion of capsule kinetic energy into hot spot pressure, and may result in similar ambiguity in the shape of the x-ray emission from the hot spot [22]. To explore the issue of low mode asymmetries further, experiments using x-ray backlighters are currently being conducted on NIF to measure the implosion shape both in-flight [11] and at stagnation using Compton radiography [21].

As discussed, implosions with a significant P_4 asymmetry can have a very apparent but "false" P_2 asymmetry in GXD images. We find that attempting to correct this "false" P_2 by increasing laser power to the hohlraum waist [18] can lead to a round GXD image even though the correction actually produces a more distorted DT fuel ice layer. This is

depicted in fig. 4 for the case of a DT layered capsule where we applied and empirically adjusted a P_2 flux asymmetry, in addition to the original P_4, in order to make the synthetic GXD image appear round. Fig. 4(c) quantifies a related effect; as the applied P_2 flux is increased in order to reduce the "false" GXD a_2 towards zero, there is a marked additional reduction in sensitivity to a_4 (relative to that shown in Fig. 3). This suggests that attempts to tune the hohlraum to eliminate a "false" P_2 can have the unintended consequence of exacerbating overall asymmetry. Other information, such as comparison of the widths of images taken from both the polar and equatorial lines of sight [23] need to be taken into consideration. These simulations show that when a hotspot has a positive but pure P_4 asymmetry the equatorial image width is larger than the width in the polar image (for negative P_4 this is reversed). This could be used to identify an implosion where the measured P_2 may be caused by a dominant P_4 asymmetry. However, our simulations also show us that the empirically but incorrectly tuned implosion of fig. 4 would have a polar image width that is equal to the equatorial image width, further misleading us into thinking that we had engineered an approximately spherical implosion. A corollary of figure 4, is that it is possible to create imploded configurations which appear to be symmetric in the GXD but, in fact, are significantly asymmetric and have significantly reduced performance in comparison to equivalent spherical implosions because a large fraction of the imploding shell's kinetic energy remains unstagnated. It is for these reasons that experimental techniques to take 2D backlit images of the capsule in-flight [11], and the cold fuel at stagnation [21] have been under development and are now beginning to provide experimental data, these additional diagnostics should eliminate this possibility.

In summary, numerical simulations have been used to examine the sensitivity of implosions similar to those currently taking place on NIF to low-mode flux asymmetries. It is shown that Legendre polynomial P_4 flux modes induce P_4 shape modes at the time of capsule stagnation. The largest P_4 amplitudes can cause up to 50% of the capsule kinetic energy to remain unconverted to hot spot and DT ice internal energy, in turn reducing the neutron yield by up to 15×. Simulated x-ray images of the hot spot self-emission show reduced sensitivity to the positive P_4 mode, instead the images appear to have a pronounced oblate P_2 shape. Attempting to correct for this apparent P_2 distortion can further distort the implosion while creating x-ray images which appear round and self-consistent from both equatorial and polar directions. This further reduces the sensitivity to the P_4 mode making

a quantitative evaluation of the hot spot a_4 ambiguous. Long wavelength asymmetries may be playing a significant role in the observed yield reduction of NIF DT implosions relative to detailed post-shot 2D simulations.

---

* Robbie.Scott@stfc.ac.uk; Also visiting scientist at Lawrence Livermore National Laboratory, Livermore, CA 94551, United States of America, and Department of Physics, The Blackett Laboratory, Imperial College London, Prince Consort Road, London, SW7 2AZ, United Kingdom. The authors thank M.H. Key and C. Cerjan for useful discussions, the staff of NIF and Livermore Computing.

[1] J. D. Lindl *et al.*, Physics of Plasmas **11**, 339 (2004).

[2] N. Basov, Edward teller lectures (1991).

[3] J. NUCKOLLS *et al.*, Nature **239**, 139 (1972).

[4] S. W. Haan *et al.*, Physics of Plasmas **18**, 051001 (2011).

[5] D. S. Clark *et al.*, Phys. Plamas **17**, 052703 (2010).

[6] D. A. Callahan *et al.*, Journal of Physics: Conference Series **112**, 022021 (2008).

[7] M. Abramowitz and I. A. Stegun, *Handbook of Mathematical Functions with Formulas, Graphs, and Mathematical Tables*, volume pp. 331-339 and 771-802, Dover (1972).

[8] V. A. Thomas and R. J. Kares, Phys. Rev. Lett. **109**, 075004 (2012).

[9] M. M. Marinak *et al.*, Physics of Plasmas **8**, 2275 (2001).

[10] L. M. Barker and R. E. Hollenbach, Journal of Applied Physics **43**, 4669 (1972).

[11] D. G. Hicks *et al.*, Physics of Plasmas **17**, 102703 (2010).

[12] R. M. More *et al.*, Physics of Fluids **31**, 3059 (1988).

[13] O. S. Jones, Private Communication, (2012).

[14] L. Rayleigh, *Scientific Papers*, Cambridge University Press, Cambridge, England (1900).

[15] G. I. Taylor, *The Instability of Liquid Surfaces when Accelerated in a Direction Perpendicular to their Planes. I*, Proc. R. Soc. London, Ser. A (1950).

[16] D. S. Clark *et al.*, Physics of Plasmas **18**, 082701 (2011).

[17] B. K. Spears *et al.*, Physics of Plasmas **19**, 056316 (2012).

[18] S. H. Glenzer *et al.*, Science **327**, 1228 (2010).

[19] D. Clark *et al.*, Physics of Plasmas *(Submitted)* (2012).

[20] P. Spinger and C. Cerjan, in *IFSA Proceedings* Bordeaux, France (2011).

[21] R. Tommasini *et al.*, Physics of Plasmas **18**, 056309 (2011).

[22] B.K. Spears, Private Communication, (2012).

[23] L.R. Benedetti, *APS DPP Proceedings*, Providence, RI, United States (2012).

Prepared by LLNL under Contract DE-AC52-07NA27344.